mathematics

MDPI

Article

Navigating the Dynamics of Squeeze Film Dampers: Unraveling Stiffness and Damping Using a Dual Lens of Reynolds Equation and Neural Network Models for Sensitivity Analysis and Predictive Insights

Haobo Wang [1], Yulai Zhao [1,*], Tongguang Yang [1], Zhong Luo [1,2] and Qingkai Han [1,2]

[1] School of Mechanical Engineering & Automation, Northeastern University, Shenyang 110819, China; hbwang@stumail.neu.edu.cn (H.W.); 2190001@stu.neu.edu.cn (T.Y.); zhluo@mail.neu.edu.cn (Z.L.); qk.han@hotmail.com (Q.H.)
[2] Key Laboratory of Vibration and Control of Aero-Propulsion System Ministry of Education, Northeastern University, Shenyang 110819, China
* Correspondence: ylzhao@stumail.neu.edu.cn

Abstract: The squeeze film damper (SFD) is proven to be highly effective in mitigating rotor vibration as it traverses the critical speed, thus making it extensively utilized in the aeroengine domain. In this paper, we investigate the stiffness and damping of SFD using the Reynolds equation and neural network models. Our specific focus includes examining the structural and operating parameters of SFDs, such as clearance, feed pressure of oil, rotor whirl, and rotational speed. Firstly, the pressure distribution analytical model of the oil film inside the SFD based on the hydrodynamic lubrication theory is established, as described by the Reynolds equation. It obtained oil film forces, pressure, stiffness, and damping values under various sets of structural, lubrication, and operating parameters, including length, clearance, boundary pressure at both sides, rotational speed, and whirling motion, by applying difference computations to the Reynolds equation. Secondly, according to the significant analyses of the obtained oil film stiffness and damping, the following three parameters of the most significance are found: clearance, rotational speed, and rotor whirl. Furthermore, neural network models, including GA-BP and decision tree models, are established based on the obtained results of difference computation. The numerical simulation and calculation of these models are then applied to show their validity with all given parameters and the three significant parameters separately as two sets of model input. Regardless of either set of model inputs, these established neural network models are capable of predicting the nonlinear stiffness and damping of the oil film inside an SFD. These sensitive parameters merely require measurement, followed by the utilization of a neural network to predict stiffness and damping instead of the Reynolds equation. This process serves structural enhancement, facilitates parameter optimization in SFDs, and provides crucial support for refining the design parameters of SFDs.

Keywords: SFD; oil film pressure distribution; stiffness; damping; neural network model

MSC: 37M05

check for updates

Citation: Wang, H.; Zhao, Y.; Yang, T.; Luo, Z.; Han, Q. Navigating the Dynamics of Squeeze Film Dampers: Unraveling Stiffness and Damping Using a Dual Lens of Reynolds Equation and Neural Network Models for Sensitivity Analysis and Predictive Insights. *Mathematics* **2024**, *12*, 771. https://doi.org/10.3390/math12050771

Received: 19 December 2023
Revised: 3 February 2024
Accepted: 8 February 2024
Published: 5 March 2024

1. Introduction

Squeeze film dampers (SFDs) can effectively reduce the vibration of a rotor system at critical speeds, so they have been widely used in the field of aeroengines. The stiffness and damping of an oil film are important characteristic parameters of SFDs, which are seriously influenced by the structural and working parameters of SFDs. The relationship between damping and stiffness and the dynamic load, rotational speed in the shaft, static eccentricity, and journal trajectory is found using theory and experiments [1–4]. For example, Fu [3] found that uncertainties in the inter-shaft bearing stiffness and speed ratios generally influence the modal characteristics and dynamical behaviors of the dual-rotor system. The quantitative effects of the oil film length and gap are compared, and factors such as structural characteristics and working variations of SFD are considered, including lubricating cavities, gas suction, sealing forms, oil inlet holes, and oil groove forms. Siew [5] proposed that the damping of SFDs is related to the viscosity of lubricating oil. Zhang [6] used the finite difference method to analyze the dynamic parameters such as oil film pressure distribution, bearing capacity, oil film stiffness, and damping characteristics of SFD.

Mathematical modeling is pivotal in scientific and engineering disciplines, providing a structured framework for analyzing complex systems and phenomena. According to Isaac Lare Animasaun [7], its significance lies in its ability to quantitatively represent real-world scenarios, facilitating prediction, optimization, and a deeper understanding of intricate relationships within diverse fields. Keir Harvey Groves and Philip Bonello [8] developed a finite difference method using Chebyshev polynomial fitting to identify the Reynolds equation, which can quickly solve the transient value of oil film pressure distribution and realize the consideration of cavitation, oil inlet, oil film pressure analysis for oil inlet, face seal, and the variation of oil supply pressure.

If SFDs are not designed properly, the nonlinear condition of oil film stiffness will occur, and damping will be affected. The research on the mechanism of the nonlinear stiffness and damping of SFDs is relatively clear now. Based on the assumption of incompressible fluid in the oil film, the oil film distribution of SFD obtained by solving the Reynolds equation with short bearings and Sommerfeld oil film boundary conditions has instantaneous displacement and velocity dependence [9–11]. It uses the finite difference method to analyze the fluid–structure interaction dynamics of the oil film and the embedded elastic ring and obtains the direct stiffness and damping coefficient, as well as the cross stiffness and damping coefficient of the SFD, which has the characteristics of hard nonlinearity [12]. Based on the Reynolds equation, Gu [13] studied the nonlinear characteristics of SFDs using the two-coefficient method. The results show that the variation of the damping coefficient of SFD is nonlinear. Gunter and Allaire [14,15] used the rotor unbalance as the design parameter of SFDs in SFD design and found that when the eccentricity ratio is greater than 0.4, SFDs have nonlinear characteristics. Cao [16,17] used the finite difference method to solve the Reynolds equation and calculated the oil film pressure of the SFD, thereby further obtaining the equivalent stiffness and damping and using the finite element method to calculate the elasticity under the premise that the floating ring does not rotate. The Reynolds equation in generalized polar coordinates of the inner and outer oil films is derived from the relationship between the stiffness of the floating ring and the eccentricity. Gu [18] proposed an SFD (VPSFD) with controllable structural parameters, which replaced the cylindrical journal and outer ring with a conical structure with a change in the radial clearance and constant. By keeping the inner cone of the damper, the radial clearance of the cone can be changed and controlled in real time by changing the axial position of the outer cone of the oil film. Liu [19] studied the amplitude–frequency characteristics of the elastic bearing stiffness, oil film gap, and other parameters of the centering SFD and obtained the optimal design method of the SFD. Chu [20] found that when the oil supply pressure and static eccentricity ratio increase, due to the highly nonlinear characteristics of the oil film force, the damping of the rotor system increases, but it also causes a large drift in the resonance position. At present, there are still some problems in the application of the above research results in engineering design, mainly because the relationship between the dynamic characteristic parameters of SFD to the structure and working parameters cannot be directly established due to the lack of clearance, the pressure boundary, and the different oil supply pressures. The influence sensitivity law and the working parameters are mainly rotational speed, whirling momentum, and so on.

Considering the fact that the commonly used SFDs are of a short journal structure and the oil film state during operation varies greatly and is seriously affected by the rotor motion, it is necessary to carry out a sensitivity analysis of the key parameters and establish a quick computational analysis method for the nonlinearity of SFD characteristic parameters, which cannot be limited to the elastic flow pressure differential equation or finite difference numerical methods. The commonly used SFDs are all short journal structures [21–23], and the variation in oil film during the working process is seriously affected by the rotor.

The nonlinear fast computational analysis method cannot be limited to elasto-hydrodynamic differential equations or finite difference numerical methods. As mentioned above, the oil film force formula and nonlinear dynamic model of SFD are complicated mathematical expressions, and it is difficult to deal with these important design parameters after sensitivity analysis. Therefore, the introduction of a surrogate model based on a neural network can well establish the relationship between the important parameters and the dynamic characteristics to achieve high-precision prediction of the damper dynamic parameters.

The application of neural network technology to the field of dynamics, especially for the dynamic analysis and dynamic design of SFD, has important innovations, especially in the aspects of nonlinear parameter identification of SFD and multi-objective optimization of structural design. M. Ananda Rao and J. Srinivas [24] proposed a BP algorithm to train the input and output data of a supervised multi-layer neural network model for the nonlinear model determination problem associated with the rotor axis trajectory and oil film force. The intelligent algorithm of data-driven rotor motion response and oil film force as neural network output under different bearing parameters is derived. Philip Bonello [25,26] used a neural network to analyze SFD modeling based on experimental data. Some factors that are difficult to model (such as geometric defects, compressibility, and cavitation effects) can be considered. The established multi-input and multi-output (input is shaft displacement and rotational speed; the output is oil film pressure and force) damping force model considering the full range of clearance changes is relatively accurate and reasonable. It can characterize the nonlinear function relationship between force, shaft displacement, and rotational speed, as well as unpredictable nonlinear behaviors such as jumps and non-synchronous vibrations when the load is large.

However, these studies based on neural networks do not focus on the dynamic characteristics and working conditions of SFD in engineering design. Previously, some parameters were found to affect the dynamic characteristics of SFDs using the Reynolds equation. But there are the following three research questions:

1. No one has studied the parameters that affect SFDs based on the dynamic characteristics of SFDs.
2. Some parameters affecting SFD are difficult to obtain in practical engineering applications.
3. The single neural network model based on multiple parameters cannot perfectly adapt to the rotor system at different rotational speeds.

It is necessary to find the sensitive parameters that affect the dynamic characteristics of SFDs using the Reynolds equation and neural networks and realize the prediction of SFD stiffness and damping through a small number of key parameters, which lays a foundation for engineering practice.

The main contributions are generalized as follows:

1. A differential equation analysis model is established based on the hydrodynamic lubrication theory for SFDs. This model considers structural parameters (length and clearance amount), state parameters (boundary pressure at both ends and oil pressure), and working parameters (rotational speed and whirling) within a defined range.
2. The peak pressure, stiffness, and damping of the SFD are determined by the differential equation. This involves conducting parametric correlation analysis to identify relationships and understand their impact on pressure distribution and stiffness damping.
3. Finally, a neural network is used to predict crucial structural parameters and damper dynamics characteristics. The prediction results of different models under different rotor system states are analyzed to determine some reasonable prediction models. These models allow for fast and highly accurate predictions, facilitating the design process.

2. Model and Numerical Methods

The working principle of SFD is that a small gap is reserved between the bearing outer ring and the bearing seat, the lubricating oil is passed into the oil, and the oil film is formed. The ends of some dampers are equipped with end-sealing rubber rings to prevent a large amount of oil leakages from the end face. When the end seal is used, pressure builds up inside and outside the cavity. The rotor is running, the journal will be whirled to drive the bearing outer ring movement, and the oil film will be squeezed, and then the damping and vibration reduction effect will be produced. This is shown in Figure 1a.

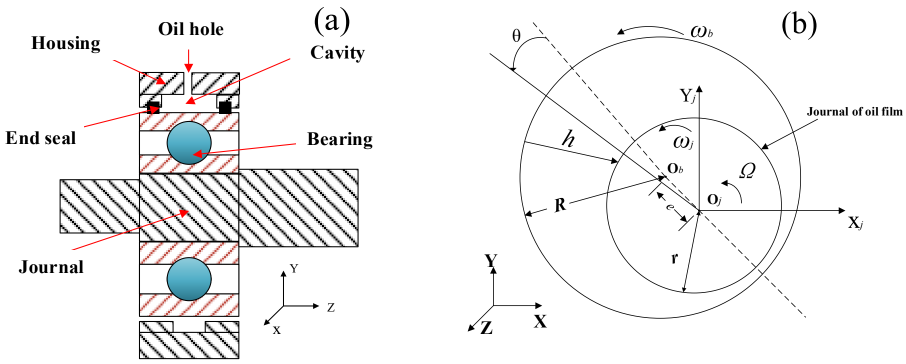

Figure 1. Typical structure of SFD and SFD-rotor system. (**a**) Installation of the SFD system. (**b**) Schematic of the SFD system.

Before establishing the Reynolds equation for SFDs, it is necessary to refer to the theory of hydrodynamic lubrication, which relies on the relative motion between a pair of solid friction surfaces to generate pressure in the lubricating fluid film between solids to withstand external loads and avoid contact between solids, thereby reducing friction resistance and protecting the solid surface.

Some assumptions need to be made before establishing the Reynolds equation of a squeeze oil film damper with hydrodynamic lubrication theory:

1. Ignore the fluid inertia force.
2. The oil film is considered an incompressible fluid.
3. The oil film viscosity coefficient is constant and does not consider the effect of temperature.
4. The oil film pressure is constant along the thickness direction and does not consider the effect of temperature.

With reference to the hydrodynamic lubrication theory, the working principle of the SFD necessitates the establishment of a coordinate system, as illustrated in Figure 1b. O_b denotes the center of the outer ring of the oil film and O_j denotes the center of the journal. The remaining variables also include the journal feed eccentricity distance (e), the oil film thickness (h), the journal radius (R), the radius of the journal of oil film (r), and the oil film ring and journal of oil film angular velocity are ω_b and ω_j. θ is the angular coordinate, and the oil film thickness is at its minimum when θ = 0. Ω is the journal precession angular velocity.

Reynolds equation for SFD based on the hydrodynamic lubrication theory:

$$\frac{\partial}{\partial\theta}\left(h^3\frac{\partial p}{\partial\theta}\right) + R^2\cdot\frac{\partial}{\partial z}\left(h^3\frac{\partial p}{\partial z}\right) = 12\cdot\mu\cdot R^2(\varepsilon\cdot\Omega\cdot\sin\theta + \dot{e}\cdot\cos\theta) \tag{1}$$

where $\dot{e} = \frac{de}{dt}$, ε is the eccentricity, $\varepsilon = e/c$. c is the clearance of oil film radius, $c = h - e\cos\theta$, p is the pressure of the film in the cavity, μ is the viscosity of oil, and z is the axial direction of SFD.

When the ratio of the length L of the damper to the diameter D is less than or equal to 0.25, the short bearing can be used for an approximate solution when the two ends are not sealed. According to (1), it can be concluded that

$$\frac{\partial}{\partial z}\left[(1+\varepsilon\cos\theta)^3\frac{\partial P}{\partial z}\right]=\frac{12\mu}{c^2}(\varepsilon\Omega\sin\theta+\dot{\varepsilon}\cos\theta) \tag{2}$$

The eccentricity (ε) and the rate of change in the eccentricity and pressure angles do not change when the journal is moving in the bearing, and the axis lines of both are always kept parallel. Based on the above assumptions and Figure 1, taking the central section of the damper as a reference, the integral limit is taken from the effective length of the damper, and the boundary condition is the pressure of the inner and outer cavity. When there is an end seal in the SFD, as shown in Figure 1a, the pressures on the left and right ends of the end seal are p_1 and p_2.

The z in Equation (1) is integrated twice, with limits taken from $-$L/2 to L/2. If the boundary condition Z = $-$L/2, p = p_1, when Z is equal to L/2, p = p_2. p_1 and p_2 will be discussed in detail later.

As shown in Figure 2.

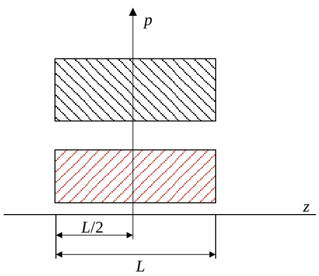

Figure 2. Short bearing integral calculation approximate oil film pressure distribution.

$$p(\theta,z)=-\frac{6\mu}{c^2(1+\varepsilon\cos\theta)^3}(\varepsilon\Omega\sin\theta+\dot{\varepsilon}\cos\theta)\left(\frac{L^2}{4}-z^2\right)+(p_2-p_1)\frac{z}{L}+\frac{1}{2}(p_2-p_1) \tag{3}$$

When there is no end seal in the SFD, the oil pressure at both ends is equal to atmospheric pressure, and the pressure of the inner and outer oil chambers is equal. The oil film distribution pressure can be obtained as follows:

$$p(\theta,z)=-\frac{6\mu}{c^2(1+\varepsilon\cos\theta)^3}(\varepsilon\Omega\sin\theta+\dot{\varepsilon}\cos\theta)\left(\frac{L^2}{4}-z^2\right) \tag{4}$$

where L is the film width and Ω is the shaft diameter feed angular speed. In synchronous whirling, the journal whirling angular velocity Ω is equal to the rotor rotation angular velocity.

The radial and tangential forces of the SFD are obtained by integrating the above equation as follows:

$$\begin{cases} F_{\mathrm{r}}=\frac{\mu RL^3}{c^2}\left[\frac{2\Omega\varepsilon^2}{(1-\varepsilon^2)^2}+\frac{\pi}{2}\cdot\frac{\dot{\varepsilon}(1+2\varepsilon^2)}{(1-\varepsilon^2)^{5/2}}\right] \\ F_{\mathrm{t}}=\frac{\mu RL^3}{c^2}\left[\frac{\pi\Omega\varepsilon}{2(1-\varepsilon^2)^{3/2}}+\frac{2\varepsilon\dot{\varepsilon}}{(1-\varepsilon^2)^2}\right]+(p_1+p_2)LR \end{cases} \tag{5}$$

The above equation can be decomposed into x-y coordinates. Let the SFD forces in the horizontal and vertical directions for the journal at the center position (0, 0) and (x, y) position be

$$\begin{cases} F_x = -\mu R L^3 \left[\frac{\pi \dot{x}}{2(c^2-x^2-y^2)^{3/2}} + \frac{3\pi x(x\dot{x}-y\dot{y})}{2(c^2-x^2-y^2)^{5/2}} + \frac{2\dot{y}\left(x^2+y^2\right)^{1/2}}{\left(c^2-x^2-y^2\right)^2} - \frac{4y(x\dot{x}+y\dot{y})}{\left(c^2-x^2-y^2\right)^2\left(x^2+y^2\right)^{1/2}} \right] \\ F_y = -\mu R L^3 \left[\frac{\pi \dot{y}}{2(c^2-x^2-y^2)^{3/2}} + \frac{3\pi y(x\dot{x}-y\dot{y})}{2(c^2-x^2-y^2)^{5/2}} - \frac{2\dot{x}\left(x^2+y^2\right)^{1/2}}{\left(c^2-x^2-y^2\right)^2} + \frac{4x(x\dot{x}-y\dot{y})}{\left(c^2-x^2-y^2\right)^2\left(x^2+y^2\right)^{1/2}} \right] \end{cases} \tag{6}$$

The oil film stiffness coefficient K and damping coefficient C of SFD are expressed as

$$K_0 = -\frac{F_r}{e}\ C_0 = -\frac{F_t}{e\Omega} \tag{7}$$

The corresponding stiffness and damping coefficients are

$$K_0 = \frac{\mu R L^3}{c^3} \cdot \frac{2\Omega\varepsilon}{\left(1-\varepsilon^2\right)^2} \quad C_0 = \frac{\mu R L^3}{c^3} \cdot \frac{\pi}{2\left(1-\varepsilon^2\right)^{3/2}} \tag{8}$$

According to the above content, the derivation calculation process is as follows (Algorithm 1):

Algorithm 1: Input: μ, r, L, c, P_1, P_2, Ω, e, ε. **Output**: p, K_0, C_0.

1. Initialize: Set μ, r, L, P_1, P_2, $\Omega \rightarrow$ data from measurement;
2. **while** ($e < c$) do;
3. prior z $\leftarrow$ $[-L/2, L/2]$;
4. posterior φ $\leftarrow$ $[0, 2\pi]$
5. else $p \leftarrow$ zeros(φ, z)
6. deterministic representation m $\leftarrow$ length (z)
7. $n \leftarrow$ length(φ)
8. **for** j = 1: m
9. **for** i = 1: n
10. calculate (i, j) by Equation (4)
11. **end for**
12. update parameters top
13. **end while**
14. calculate K_0, C_0 by Equation (8)
15. **end**

3. Parameters Impact Analysis for Stiffness and Damping of SFD Based on the Reynolds Equation

A theoretical analysis model is used based on the principles of hydrodynamic lubrication theory to examine structural parameters such as eccentricity (ε) and clearance (c), as well as state parameters including oil pressure at both ends and working parameters like rotational speed and whirling motion within a specified range. This will obtain the pressure peak, and the stiffness and damping values of SFD are analyzed for parameter correlation using the numerical solution of differential equations.

A rotor system using a support structure with a squeeze film damper and its parameters are shown in Table 1.

3.1. Impact Analysis of State Parameters

The oil supply method of SFDs is generally either through the oil hole or a circumferential sink. The bearing has a strict left and right axial seal; that is, the left side is the positioning limit for the outer ring installation, and the right side has a seal. Therefore, there are both pressures on the left and right sides of the seal. Usually, for the circumferential oil supply method, it is assumed that the oil pressure in the oil tank is constant, and with the continuous operation of the rotor system, the oil pressure at the left and right ends of the SFD will change continuously.

Table 1. Parameter of SFD.

Parameter	Data
Radius of journal (mm)	42.5
Viscosity oflubricating oil (Pa·s)	0.0153
Eccentricity	0.1-0.9
Oil pressure p_1 and p_2 (MPa)	0.3
Oil film width (mm)	19
Clearance (mm)	0.2–0.5
Initial frequency (Hz)	50
Eccentric distance (mm)	0.03

3.1.1. Effect of Pressure Distribution with Oil Pressure Variation

At the initial state, the clearance (c) is 0.2 mm, the eccentricity (ε) is 0.9, and both ends of the oil pressure are 0.3 MPa; the pressure distribution is shown in Figure 3. The angular pressure distribution is 0 near the maximum oil film thickness (180°); from 0° to 180° (or 180°–360°, with respect to the direction of feed) is the negative pressure zone, and 180–360° is the positive pressure zone (when the cavitation effect is not considered, the pressure in the negative pressure region is usually set as 0; it is considered that the oil film has no bearing capacity in the negative pressure region). We need to consider the cavitation effect in the negative pressure zone when the oil film pressure is greater than the cavitation. When the oil film is under pressure, it is considered that the oil film still has a carrying capacity, and when the oil film is under pressure, the force is less than the cavitation pressure, and the oil film loses its bearing capacity.

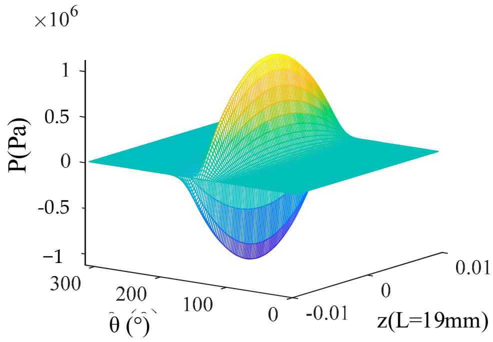

Figure 3. Oil film pressure distribution (including negative pressure).

Considering the fact that the pressure at the left end is greater than the pressure at the right end, p_1 = 0.3 MPa and p_2 = 0.1 MPa; the pressure distribution is shown in Figure 4.

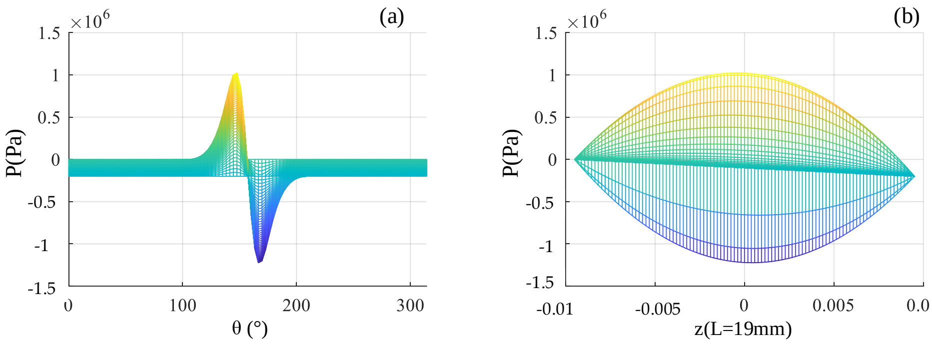

Figure 4. Pressure distribution when $p_1 > p_2$. (**a**) Angular pressure distribution; (**b**) axial pressure distribution.

Then, consider the fact that the pressure at the right end is greater than the pressure at the left end when p_1=0.1 MPa and p_2=0.3 MPa, and the pressure distribution is shown in Figure 5.

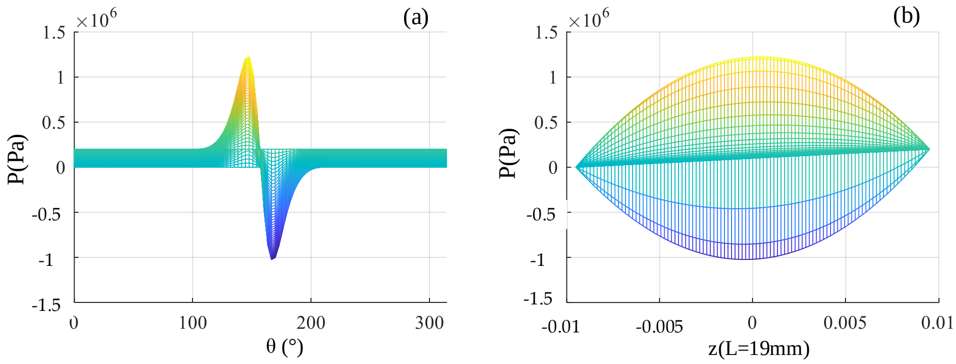

Figure 5. Pressure distribution when $p_1 < p_{2.}$ (**a**) Angular pressure distribution; (**b**) axial pressure distribution.

As can be seen from the figure, when the oil pressure appears different, the axial oil film pressure changes, and the higher the oil pressure, the greater the oil film pressure. Therefore, according to the calculation of the Reynolds equation, the oil supply pressure at both ends will affect the pressure distribution of the SFD.

3.1.2. The Effect on Stiffness and Damping

The oil film stiffness and damping when the oil pressure is different between the left and right ends are shown in Table 2.

Table 2. Results of oil film stiffness and damping under different pressure conditions.

Condition	K (N/m)	C (N·s/m)
$p_1 > p_2$	1.39×10^6	5.57×10^4
$p_1 < p_2$	1.39×10^6	5.57×10^4

As can be seen from the table, when the oil pressure at both ends is different, it has no effect on the oil film stiffness and damping. It can be observed that the oil pressure at both ends is not impacted by the stiffness and damping of SFDs.

3.2. Impact Analysis of Structural Parameters

The radius difference between the outer ring of the bearing and the seat of the plate, i.e., the clearance (c), will lead to a change in the value through machining and assembly; at the same time, this makes the eccentricity (ε) have variation.

3.2.1. The Effect on Pressure Distribution

The pressure distribution is in the range of 0.1–0.9 for ε and 0.2 mm–0.5 mm for clearance (c). Taking it as 0.5 mm, the different pressure distributions are shown in Figure 6a. When the center of the shaft makes a circular motion, the oil film pressure distribution along the axial direction is approximately parabolic, and the oil film pressure is at its maximum near the center. When the eccentricity (ε) = 0.9, the pressure distribution of different clearances is shown in Figure 6b. It can be determined that both the clearance (c) and eccentricity (ε) have an effect on the pressure distribution of the SFD.

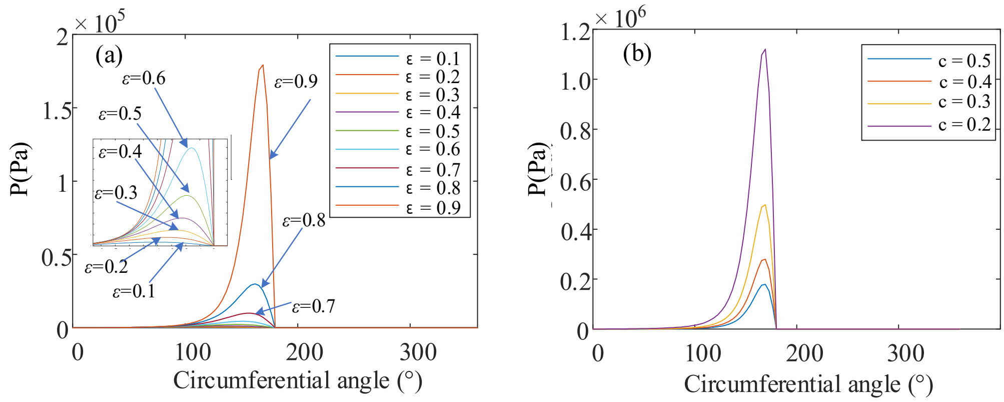

Figure 6. Pressure distribution under different eccentricity and oil film clearances (**a**) when clearance (c) = 0.5 mm and (**b**) when eccentricity (ε) = 0.9.

3.2.2. The Effect on Stiffness and Damping

When the eccentricity and clearance change, the tendency of stiffness and damping to change with the eccentricity and clearance can be obtained, as shown in Figures 7 and 8.

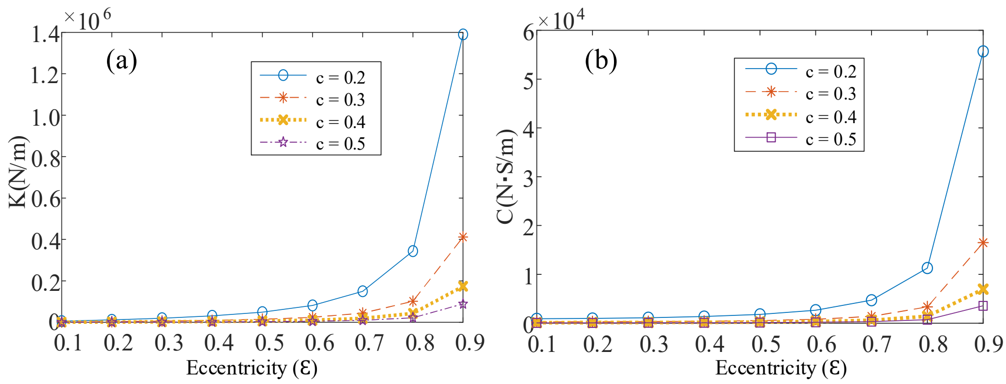

Figure 7. The variation trend of stiffness and damping with eccentricity; (**a**) stiffness; and (**b**) damping.

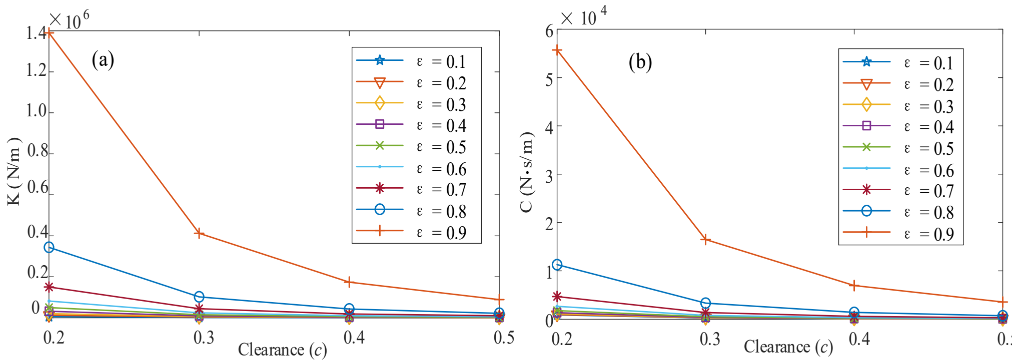

Figure 8. Variation of stiffness and damping with oil film clearance: (**a**) stiffness; (**b**) damping.

It can be seen from the above trend graph that, with the variation in clearance and eccentricity, the oil film stiffness and damping have strong nonlinear characteristics. When the eccentricity is higher than 0.7, a steep increase in stiffness and damping occurs. At the same time, the oil film gap amount for clearance (c) changes more significantly in the range interval of 0.2 mm–0.3 mm. Therefore, it can be judged that the eccentricity and oil film clearance (c) are important parameters in the corresponding range, and it is necessary to improve the damping performance of the squeeze film damper by adjusting these two parameters in the de

3.3. The Effect Analysis of Working Parameters

When the rotor system is running, the variation in the rotational speed and the whirling state generated during operation will have a certain influence on the stiffness and damping of SFDs. At the same time, during the operation of the rotor, as the rotational speed increases to different states, the journal also whirls, and its whirling state will also affect the stiffness and damping. Therefore, the working state of the rotor will be divided, considering the journal whirling state.

3.3.1. The Effect of Rotational Speed on Pressure Distribution without the Whirling State

When the rotor system rotational speed increases, the pressure distribution of the SFD will change drastically with the increase in the rotational speed. After setting the rotational frequency, the pressure distribution of the three rotational speeds can be observed, as shown in Figure 9. It can be seen from the graph that the peak pressure of the oil film increases when the rotational speed increases.

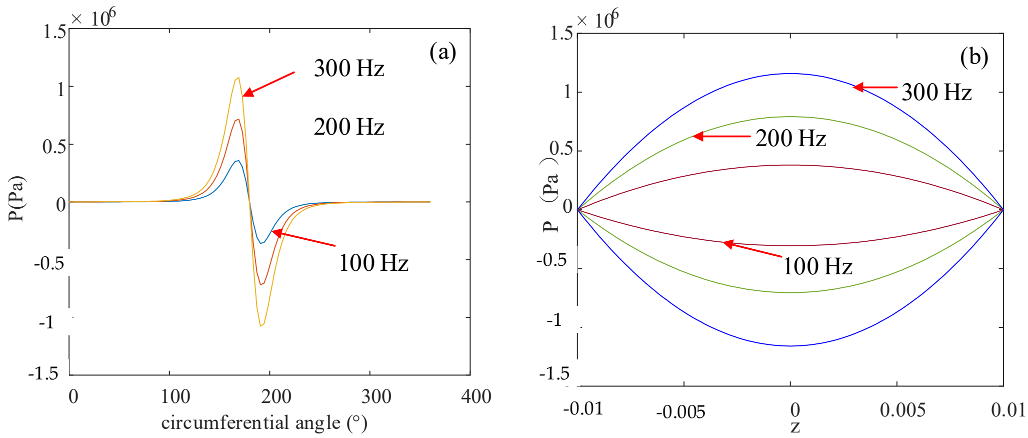

Figure 9. Oil film pressure distribution of SFD at different rotational frequencies (L = 19 mm). (**a**) Angular pressure distribution of the oil film. (**b**) Axial pressure distribution of the oil film.

3.3.2. The Effect of Rotational Speed on the Stiffness and Damping

Firstly, the oil film stiffness and damping of the SFD at different frequencies are shown in Table 3. It can be seen that when the frequency is increased, the oil film stiffness shows a linear increasing trend, while the damping does not change.

Table 3. Oil film stiffness and damping of SFD at different rotational speed.

Rotational Speed (Hz)	*K* (N/m)	*C* (N·s/m)
100	1.78×10^5	3560
200	3.56×10^5	3560
300	5.34×10^5	3560

When putting the SFD into the rotor system, this will be affected by the dynamic characteristics of the rotor system. The oil film pressure distribution, stiffness, and damping will change under different rotor rotational speeds. Due to the error in manufacturing, the centroid of each section of the rotor generally has a slight deviation from the rotation axis. When the rotor rotates, the centrifugal force caused by the above deviation will cause the rotor to produce a whirling motion, resulting in nonlinear changes in SFD stiffness and damping. The simulation model of the high-pressure rotor system with SFDs of a certain type of air engine is established [27], and according to the vibration response of different rotational speeds (including the axis trajectory), as shown in Figure 10, the first order is 280 Hz. When the rotor system works, it is accompanied by different whirling states, and when the rotational speed is below the critical rotational speed, the rotor system is in a small whirling state. When the rotational speed reaches the critical rotational speed, the amplitude of the rotor system is in a large whirling state. After the critical rotational speed, the rotor is in a medium whirling state. In the following article, the characteristics of the pressure distribution, stiffness, and damping of the oil film pressure distribution, SFD, and the different rotational speeds of the different rotational speeds are discussed.

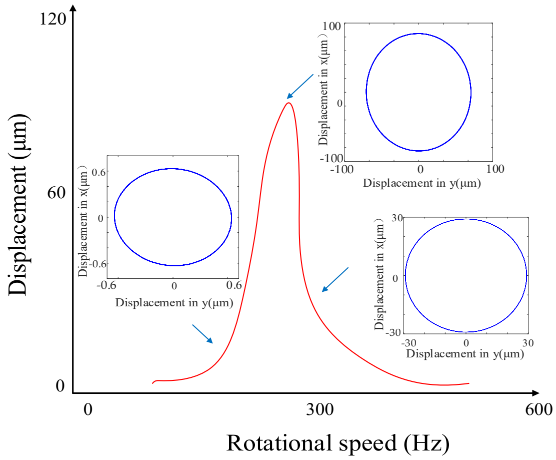

Figure 10. Vibration response in different rotational speed.

3.3.3. The Effect of the Whirling State on Pressure Distribution

When whirling occurs during rotor operation, it remains constant, and clearance (c) will change with eccentricity (ε).When the rotor is running, with the change in the rotational speed, the rotating shaft will bend and deform under the action of unbalanced torque, which will produce a whirling motion. And according to the different speed, which is only considered by the first critical speed, the following three rotor whirling conditions are considered: (1) small amplitude whirling (ε = 0.3, 130 Hz); (2) medium amplitude whirling (ε = 0.6, 280 Hz); and (3) large amplitude whirling (ε = 0.9, 220 Hz). These different conditions and parameters are shown in the Table 4. The obtained oil film pressure distribution is shown in Figure 11. It can be seen that the pressure distribution is has more of an impact and the pressure peak is higher when large amplitude whirling occurs in the rotor system.

Table 4. Three different conditions with parameters of the rotor system.

Case	Whirling	Rotational Speed (Hz)
1	ε = 0.3	130
2	ε = 0.6	280
3	ε = 0.9	220

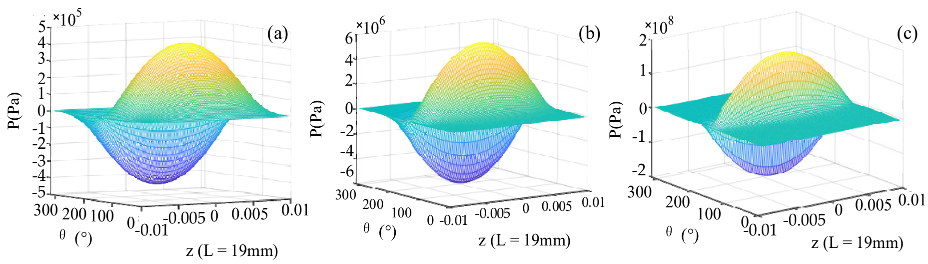

Figure 11. Oil film pressure distribution under different conditions (**a**) ε = 0.3, 130 Hz; (**b**) ε = 0.6, 280 Hz; and (**c**) ε = 0.9, 220 Hz.

As the rotational speed increases, the oil film area decreases after reaching the resonance frequency and large amplitude whirling, but the pressure increases steeply. After passing the resonance frequency, the oil film area becomes larger when medium amplitude whirling occurs and the pressure decreases gradually. Thus, it can be determined that when in a state of large whirling, the pressure distribution of the oil film has more impact. According to Equation (4), the peak value of oil film pressure is directly proportional to eccentricity. In the three cases, the maximum and minimum pressure values differ by thousands of times, which shows that eccentricity is very sensitive to the oil film pressure. Larger oil film pressure is an important prerequisite for ensuring that an SFD has sufficient damping.

3.3.4. The Effect of the Whirling State on the Stiffness and Damping

We set up three cases according to three states. We set 10 rotational speeds for each case and calculated their stiffness values as follows: (1) Case 1: e = 0.3c, 0–130 Hz; (2) Case 2: e = 0.6c, 280–600 Hz; (3) Case 3: e = 0.9c, 180–230 Hz. In these cases, the stiffness results of the SFD are shown in Figure 12.

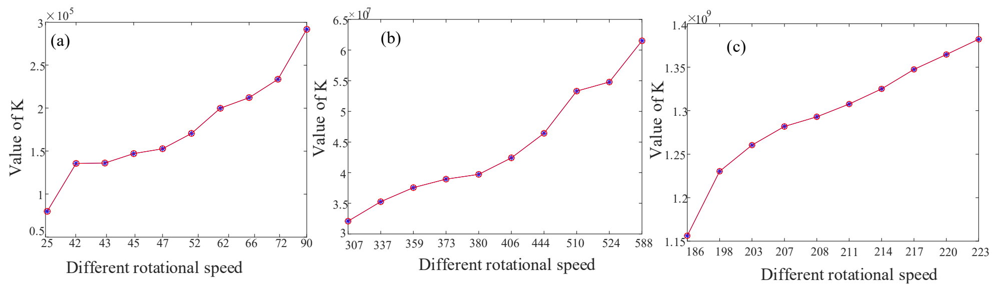

Figure 12. Three cases of the stiffness results: (**a**) Case 1; (**b**) Case 2; (**c**) Case 3.

Based on the analysis of different cases, when the whirling state of the rotor system is introduced into the calculation of the stiffness and damping of the SFD, according to Equations (7) and (8), rotor whirling mainly affects the stiffness, and the relationship between the rotational speed and the stiffness is linear, so the stiffness changes dramatically with the rotational speed.

Based on the above research, it can be concluded that the oil film force, the pressure distribution of the oil film, and the oil film stiffness and damping are analyzed and compared using the Reynolds equation. The structural parameters gap c and eccentricity will have an effect on the stiffness and damping of the SFD. In the rotor system, the rotational speed impacts the stiffness and damping of the SFD when the rotor system works without considering the whirling state. When considering the whirling state of the rotor, the variation in eccentricity causes a certain change in the oil film clearance, and the pressure distribution changes sharply so that the stiffness changes sharply. Therefore, the working parameter and the whirling of the journal at different rotational speeds will have an effect on stiffness and damping.

Therefore, in practical engineering applications, if the lubricating oil temperature is too high, this will make its viscosity decrease significantly, which, on the one hand, can lead to poor lubrication and cooling effects and, on the other hand, will weaken the squeeze film damper damping effect [28]. At the same time, the damping effect is related to the viscosity of the liquid; the larger the viscosity, the more obvious the damping effect, but the relationship is not linear [29]. When the oil viscosity (on both sides of the pressure in SFD), oil supply pressure, flow, and other parameters are difficult to measure and identify, a neural network system can be introduced using the above several parameters to complete the SFD oil film pressure distribution and stiffness analysis.

4. Parameter Analysis for Stiffness and Damping of SFDs Based on Neural Networks

Through the above sensitivity analysis of the important parameters affecting the stiffness and damping of SFDs based on the Reynolds equation, some parameters can be obtained that have the strongest influence on stiffness and damping. Then, based on neural network technology, an adaptive neural network model without artificial decision is proposed using the simulation data in the multi-input (load conditions, working conditions, and structural parameters) and multi-output (peak pressure and damping stiffness) nonlinear approaches.

The neural network model is divided into the BP neural network, the improved BP neural network based on a genetic algorithm (GA-BP), the particle swarm optimization BP network (PSO-BP), and the decision tree model. According to the Reynolds equation, the results of stiffness and damping are obtained by establishing a dynamic model and changing the values of different parameters. According to different working conditions, it is divided into three groups of data, with each group of data training sets comprising 200 groups and 10 test set groups. The test set contains different state parameters, working parameters, and structural parameters. Through the prediction of the above four models and the comparison of the error of the results, the accuracy and applicability of the model can be detected, and a nonlinear prediction model with intermediate variables of damper state parameters and multiple input and output characteristics can be established, which can be jointly driven by multiple sets of simulation data.

4.1. Data-Driven Modeling and Method

4.1.1. BP Neural Network Model

The BP neural network is the most widely used artificial neural network model. It consists of the following two processes: the forward propagation of information and the back propagation of errors. The weights and thresholds are updated by the error of the output results. Establishing the model mainly involves the following aspects: the reasonable selection of input and output parameters; the selection of the number of hidden layer intermediate nodes; and the optimization of initial weights and thresholds. It needs to select reasonable input and output parameters. Although the neural network model does not focus on specific physical processes, the research object itself has a clear physical meaning, and there is a clear physical correspondence between each output and input parameter. If the input and output parameters are randomly selected, it may provide wrong information to the neural network model. Using a correlation analysis, the input parameters can be effectively determined according to the output parameters. Nine parameters have been determined (μ, e, R, c, L, p_1, p_2, ω, and ε), including the output stiffness K and damping C two parameters. The hidden layer is 10, as shown in Figure 13.

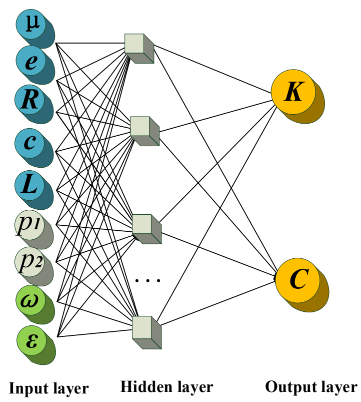

Figure 13. The structure of the BP neural network.

When the neural network has a large number of layers, the gradient information in the backpropagation algorithm will be passed back to the input layer through many layers, and each layer will be multiplied by the derivative of the activation function. If these derivatives are all less than 1, then as the number of layers increases, the gradient multiplied by the derivative will shrink and eventually become very close to 0. This causes the gradients to gradually disappear during propagation, and the weight of the shallow network cannot be effectively updated, thus making the network unable to learn effective representations and models. The gradient disappearance problem mainly occurs in deep neural networks.

To mitigate this problem, BP neural networks need to be optimized, usually by using more appropriate activation functions, batch normalization, residual chaining, or more appropriate weight initialization methods. Therefore, BP neural network optimization models GA-BP and PSO are used for comparative analysis.

The genetic algorithm (GA) is a method that searches for the optimal solution by simulating the natural evolution process. The algorithm converts the solution process of the optimal value problem into a genetic process that is similar to the genetic processes in biological evolution using mathematical methods. Compared with some conventional optimization algorithms, it usually obtains better optimization results faster. The optimization process is shown as follows: after determining the structure of the BP neural network, the initial weights and thresholds of the neural network are input into the genetic algorithm, and the error after the training of the neural network is used as the fitness value, and then the weights and thresholds of the neural network are optimized. After the optimal weight threshold is obtained, it is substituted into the training and prediction processes of the neural network. The GA-BP algorithm based on the input parameters of SFDs is shown in Figure 13. In three different states, the prediction results of the nine-parameter input GA-BP neural network prediction model are compared with the Reynolds equation simulation results in Figure 14.

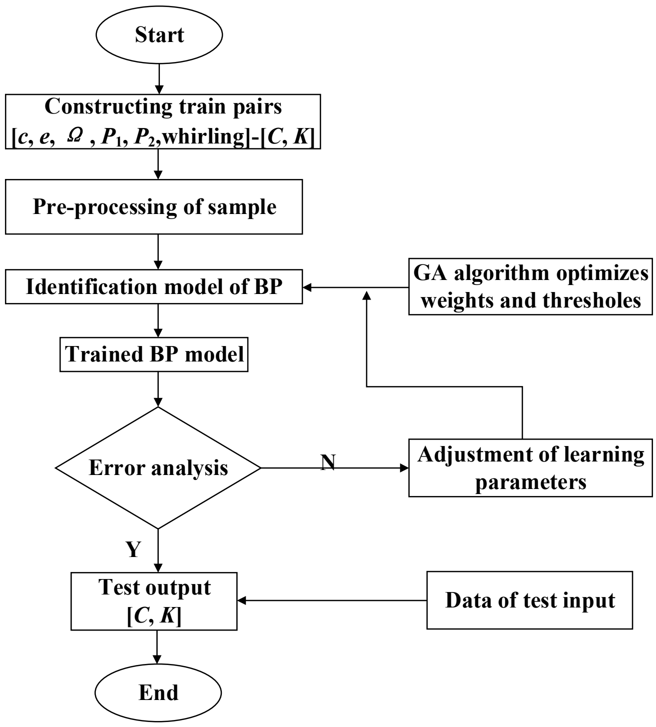

Figure 14. GA−BP based on the input parameters of SFD.

The particle swarm optimization (PSO) algorithm is a global random search algorithm based on swarm intelligence, which is proposed by simulating the migration and swarming behavior of birds in the process of foraging. It regards the individuals in the group as particles without mass or volume in the D-dimensional search space. Each particle moves in space at a certain rotational speed and gathers to its own historical best position (pbest) and the neighborhood historical best position (gbest) to realize the evolution of candidate solutions. It is simple, has a fast convergence rotational speed, has fewer setting parameters, and has other advantages. In three different states, the prediction results of the nine-parameter input PSO neural network prediction model are compared with the Reynolds equation simulation results.

4.1.2. Decision Tree Model

A decision tree is a special tree structure. It is similar to the structure of a flow chart, where each internal node represents a 'test' on an attribute, each branch represents the result of the test, and each leaf node represents a class label (the decision taken after calculating all attributes). The path from root to leaf represents the classification rule, resulting in a decision tree. Machine learning techniques that generate decision trees from data are called decision tree learning or decision trees. In machine learning, a decision tree is a prediction model that establishes a mapping relationship between predicted object attributes and object values. In data mining, a decision tree is often used, which can be used to analyze data and make predictions. In general, a decision tree contains a root node, several internal nodes, several branches, and several leaf nodes. The root node is generally used for the input; each internal node represents a judgment on the attribute; each branch represents an output of the judgment result; and finally, each leaf node represents a classification result. In the process of prediction, the decision tree model has the characteristics of better processing classification data, especially high-accuracy classification rules, and processing multi-channel input and output.

The results were compared with those obtained by the Reynolds equation and the above four neural network models to predict stiffness and damping, as shown in Figure 15. It can be seen from the figure that the stiffness prediction results of BP and its improved model in Case 1 are highly consistent with the results of the Reynolds equation. The result of the decision tree in Case 2 is better than that of PSO. But the PSO results in Case 3 are highly consistent with the results of the Reynolds equation. According to the comparison of the prediction results in the three cases, the neural network model shows that the rotational speed and eccentricity have a significant influence on the stiffness of SFDs, which is consistent with the analysis results of the Reynolds equation. Since the stiffness prediction is only carried out for different rotational speeds, the damping calculation in the Reynolds equation does not involve the rotational speed. Therefore, the damping result error is very small when the four methods are used to predict the results.

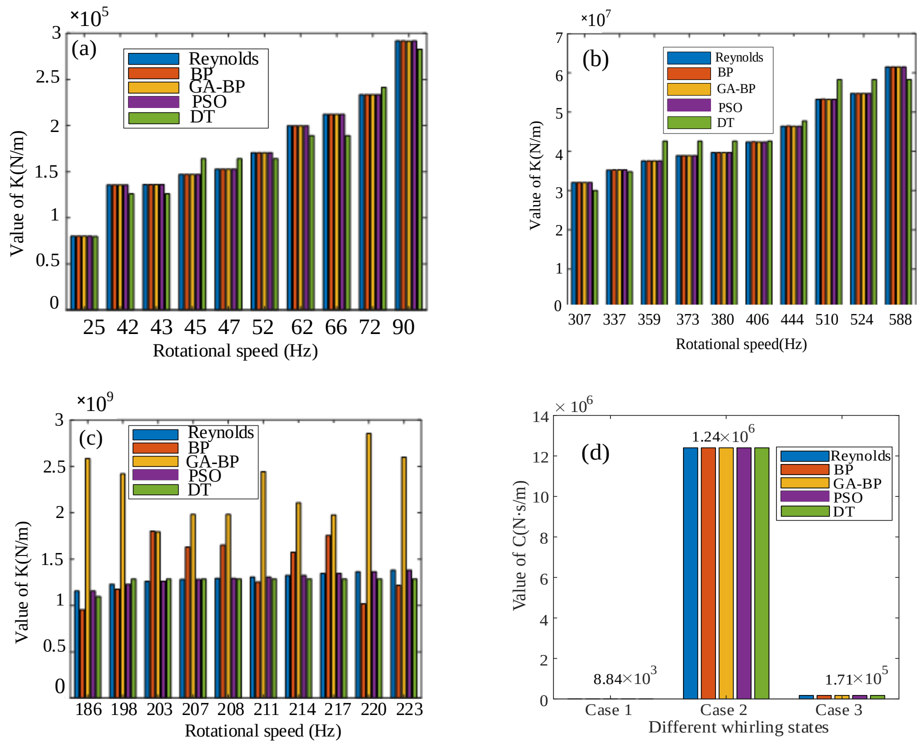

Figure 15. Comparison of stiffness prediction models (**a**) Case 1; (**b**) Case 2; (**c**) Case 3; (**d**) comparison of damping prediction models for Case 1, Case 2, and Case 3.

4.1.3. The Prediction Results of Different ε and c with the Same Rotational Speed of Rotor System

In the above Reynolds equation and the above neural network predictions, since the rotational speed has no effect on the damping, the model has limitations on the prediction of damping. Therefore, this section focuses on the prediction of stiffness and damping according to different eccentricity (ε) and clearance (c) levels when the rotational speed is constant. The stiffness and damping prediction results of each model with Case 1 and Case 2 are shown in Figure 16.

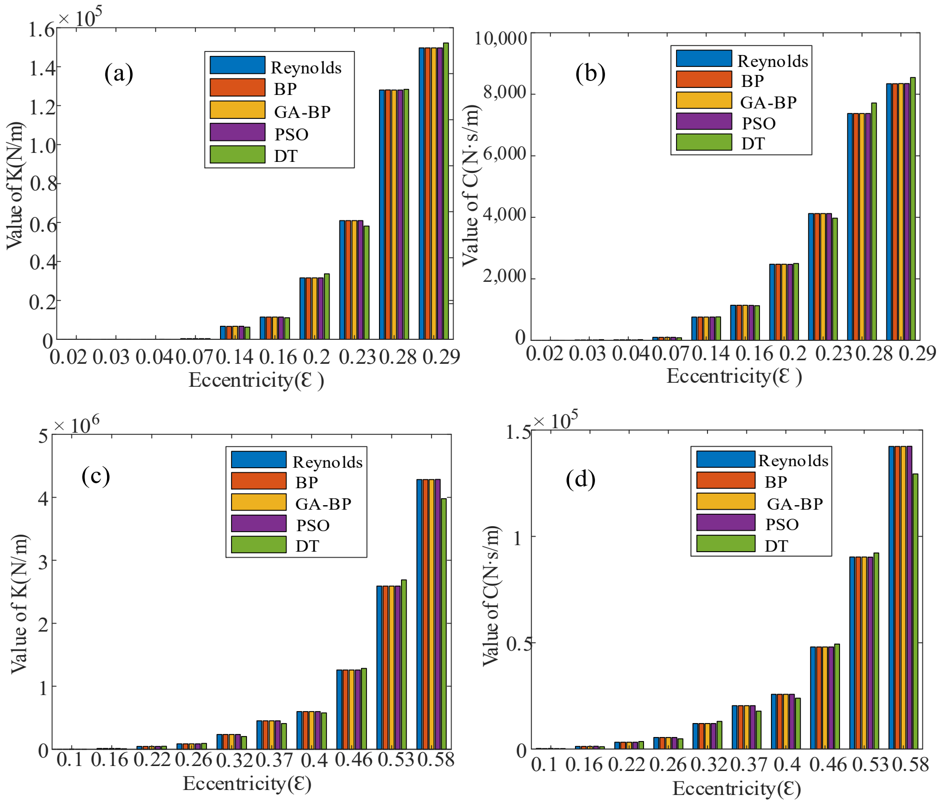

Figure 16. The stiffness and damping prediction and comparison results with all the methods. (**a**) Case 1: the stiffness; (**b**) Case 1: the results of damping prediction; (**c**) Case 2: the stiffness; (**d**) Case 2: the results of damping prediction.

The accuracy of stiffness and damping prediction in Case 3 obtained by the BP algorithm and its two improved algorithms is very low. The results obtained by the decision tree model are shown in Figure 17.

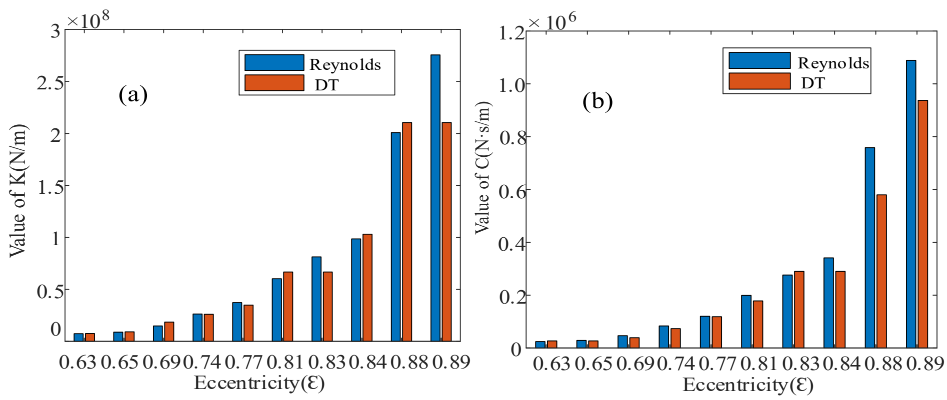

Figure 17. The results obtained by the decision tree model compared with the Reynolds theory: (**a**) stiffness; (**b**) damping.

4.2. Comparison of Results of Different Neural Network Models under Different Working Conditions

The result obtained by the Reynolds equation is defined as a real value; the result obtained by the above model is defined as a prediction value. The result obtained by the Reynolds equation for 10 different speeds in each case is $TV = (TV_1, TV_2, \ldots, TV_{10})$, and the prediction result obtained by neural network model is $PV = (PV_1, PV_2, \ldots, PV_{10})$, so the relative error at each speed is $RE_n = (TV_n - PV_n)/TV_n$. The mean relative error is $MRE_n = (RE_1 + RE_2 + \ldots + RE_{10})/10$. The mean relative error of nine parameters to K and C is shown in Tables 5 and 6.

Table 5. Mean relative error (%) of nine parameters to K in the three cases (different rotational speed).

Model	Case 1	Case 2	Case 3
BP	0.0057	0.031	0.21
GA-BP	0.0018	0.0065	0.76
PSO	0.00004	0.0096	0.0014
DT	0.06	0.02	0.03

Table 6. Mean relative error (%) of nine parameters to K and C in the three cases (same rotational speed).

Model	*K*			*C*		
	Case 1	Case 2	Case 3	Case 1	Case 2	Case 3
BP	0.23	0.04	84	0.52	1.04	39
GA-BP	0.04	0.01	13	0.08	0.02	25
PSO	2.45	0.31	31	10.2	0.88	17
DT	2.15	0.13	0.1	0.16	0.08	0.13

It can be found that the prediction results of the BP neural network and its two improved methods (GA-BP and PSO) are more accurate at low and medium rotational speeds. At high rotational speed, the prediction results of the PSO model and the decision tree model in the neural network model with nine parameter inputs are more accurate. At the same rotational speed, the prediction results of GA-BP are relatively accurate in Cases 1 and 2. The prediction results of the decision tree are relatively accurate in Case 3. Different suitable neural network models can be selected to predict the stiffness and damping of SFDs under different rotor states instead of the Reynolds equation.

4.3. Parameter Impact Analysis Based on a Neural Network Model

In practical engineering applications, the oil viscosity, internal and external oil pressures in SFD, and other parameters are not easy to measure and identify. Aiming at the difficulty of obtaining parameters such as SFD structure and working state and the influence of stiffness and damping sensitivity, the sensitivity of each parameter is identified using the Sobol method [30], as is the contribution ratio of each input parameter to the output variance.

The core idea of the Sobol method is variance decomposition [31]. It decomposes the model into a single parameter and a function of the combination of parameters, calculates the contribution of the variance of a single input parameter or input parameter set to the output variance, and then analyzes the importance of the parameters and the interactions between parameters.

Assume that the model $Y = f(x) = f(x_1, x_2, \ldots x_n)$, where $X = [x_1, x_2, \ldots x_n]$ is the parameter vector, n is the number of parameters. After Sobol sampling of the respective variables, the total variance is obtained. After decomposing it into several sub-variances, the decomposition formula is expressed as follows:

$$D(Y) = \sum_i D_i + \sum_{i \leq j} D_{ij} + \cdots + D_{12\cdots n} \tag{9}$$

where $D(Y)$ is the total variance of the model, D_i is the variance term of the ith parameter; D_{ij} is the variance term of the joint action of the ith and jth parameters; $D_{12...n}$ is the variance term for all interactions. In this paper, the first-order sensitivity S_i is used as the sensitivity index to calculate the following:

$$S_i = \frac{D_i}{D(Y)} \tag{10}$$

Based on the above stiffness and damping formula, the journal radius and oil film width of the six parameters are invariant, and the oil viscosity will change slightly during the operation of the damper. Therefore, the value range of the parameters is shown in Table 7. The sensitivity analysis results for these parameters are shown in Figure 18. It can be seen that the sensitivity of the rotational speed, eccentricity, and oil film clearance is relatively high.

Table 7. The value range of the parameters.

Variables	Oil Viscosity (Pa·s)	Clearance (mm)	Rotation (Hz)	Eccentricity
Max	0.016	0.9	600	0.9
Min	0.015	0.1	1	0.1

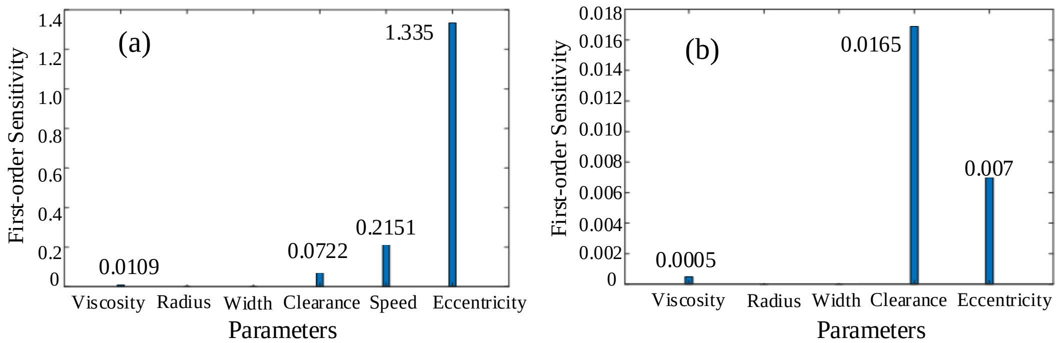

Figure 18. The sensitivity analysis results of the parameters: (**a**) stiffness; (**b**) damping.

4.4. Prediction and Comparison Results Based on Three Parameters

Only three parameters of rotational speed, clearance (c), and eccentricity (ε) are necessary to input into the neural network model according to different whirling states so as to predict stiffness and damping accurately and reasonably. The prediction and comparison results of different neural network models based on three input parameters in three cases are shown in Figure 19. Since the damping prediction results are the same as previous results, they will not be repeated here. The prediction results in Case 3 can only be made using the decision tree in the Figure 20.

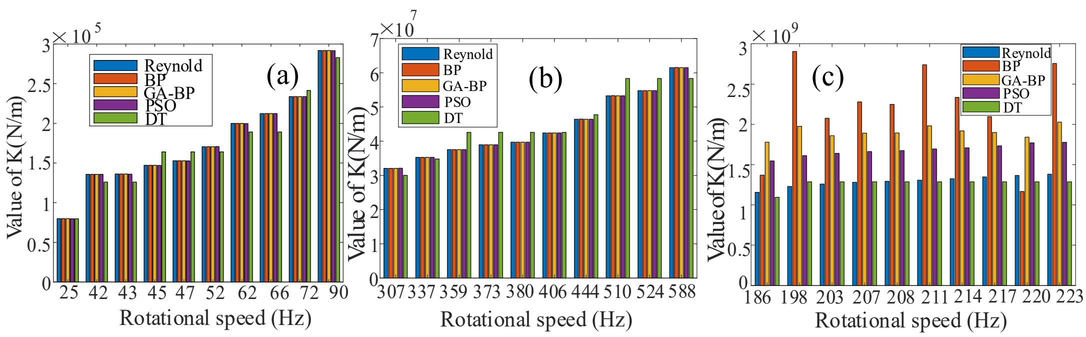

Figure 19. The prediction results of stiffness and damping of each model with same rotational speed. (**a**) Case 1; (**b**) Case 2; (**c**) Case 3.

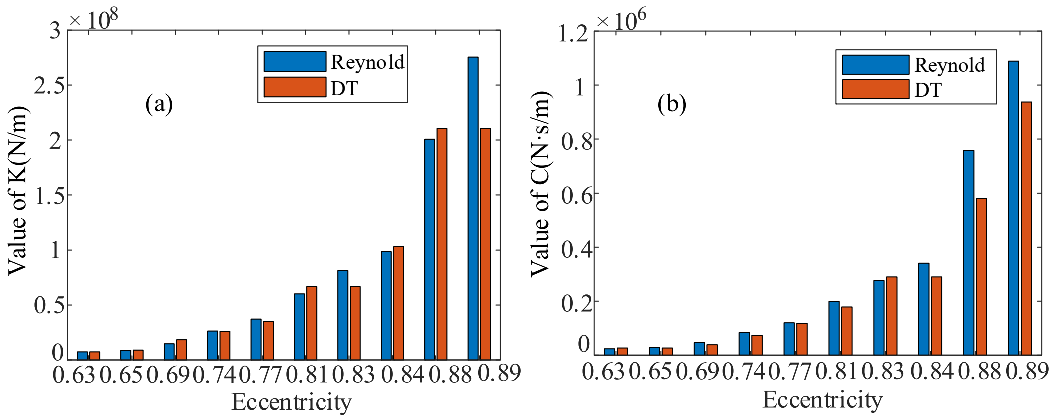

Figure 20. The results with different rotational speed in Case 3: (**a**) stiffness; (**b**) damping.

Through the difference in rotational speed and the whirling state, the neural network model can use rotational speed, clearance (c), and eccentricity (ε) as inputs and use the relatively accurate prediction model discussed above to predict stiffness and damping in three states, respectively. The results are outlined in Table 8. The prediction accuracy of the three BP methods is very low, with different rotational speeds and large amplitude whirling. The error predicted by the decision tree is relatively good, as shown in the Table 9.

Table 8. Mean relative error (%) of three parameters to K with a different rotational speed (%).

Model	Case 1	Case 2	Case 3
BP	0.00019	0.017	9
GA-BP	0.000031	0.0021	84
PSO	0.029	0.0023	13
DT	18	17	0.034

Table 9. Mean relative error (%) of three parameters to K and C with the same rotational speed.

Model	*K*			*C*		
	Case 1	**Case 2**	**Case 3**	**Case 1**	**Case 2**	**Case 3**
BP	24	13	120	31	15	25
GA-BP	0.38	0.0002	82	0.0008	0.0006	73
PSO	11	40	26	26	15	30
DT	20	70	0.1	43	64	0.13

GA-BP and decision tree methods have relatively low average relative errors for the same rotational speed and different whirling states.

It can be seen that the accuracy of the GA-BP model's prediction is further improved when only three parameters are input. Because of the particularity of the decision tree model, the results remain unchanged when three parameters are input. According to the predicted results, it can be concluded that the GA-BP model has higher accuracy when predicting stiffness in different whirling states, especially in low whirling states and medium whirling states. In the high whirling state, the prediction of the decision tree model is relatively accurate. At the same time, with large whirling, the stiffness and damping of SFDs can be effectively predicted by the prediction model established by the neural network with only three parameters, which provides a rich reference value for subsequent design approaches and calculations.

4.5. Discussion of Results

The results can be discussed using the above analysis.

1. Based on the predicted results, different neural network models can be selected to predict SFD stiffness and damping according to different states of the rotor.
2. Three parameters affecting stiffness and damping are found using the Sobol method and practical engineering applications, and stiffness and damping can be predicted using the neural network model.
3. The neural network models are used to predict the SFD's stiffness and damping of the rotor system under different states using some sensitive parameters instead of the Reynolds equation.

5. Conclusions

Firstly, a theoretical model designed to analyze the pressure distribution in SFDs is presented. The critical parameters, including the oil film force, pressure distribution, stiffness, and damping, are computed within this framework. Structural factors such as length and clearance, state-related aspects like boundary pressure and oil inlet pressure, and operational conditions such as rotational speed are taken into account during the calculation process. Then, neural network prediction models like BP and decision tree models were established based on the obtained theoretical results, incorporating all of the given parameters. Thirdly, our conclusions are as follows:

1. We found that the three most significant parameters (rotational speed, eccentricity, and clearance) are examined separately as inputs.
2. The neural network models prove effective in accurately predicting the nonlinear stiffness and damping of the SFD with different parameters. Especially for the nonlinear issue of the rotor system, different neural network models can be used for better prediction under different rotor states.
3. The GA-BP model can be used for both low speeds and critical speeds. The decision tree model can be selected for high speed.
4. Only the sensitive parameters are required to be measured and combined with the neural network to predict the stiffness and damping of SFDs instead of using the Reynolds equation.

Finally, the study in this paper will serve as a foundation for the structural enhancement and facilitation of parameter optimization in SFDs. The precise predictions obtained by the proposed approach are of significant importance, contributing to improvements in design approaches and the optimization of performance across diverse engineering applications. This methodology provides crucial support for refining the design parameters of SFD.

Author Contributions: Conceptualization, Q.H., Y.Z. and H.W.; data curation, Y.Z. and T.Y.; formal analysis, H.W.; funding acquisition, Q.H.; investigation, H.W.; methodology, Y.Z. and H.W.; project administration, Q.H.; resources, Q.H. and Z.L.; software, Y.Z.; supervision, H.W. and Y.Z.; validation, Y.Z.; visualization, H.W.; writing—original draft, H.W.; writing—review and editing, Y.Z. All authors have read and agreed to the published version of the manuscript.

Funding: This research was funded by the National Natural Science Foundation of China (grant No. 12072069).

Data Availability Statement: The datasets used and analyzed during the current study are available from the corresponding authors upon reasonable request.

Conflicts of Interest: The authors declare that they have no conflicts of interest.

References

1. Wang, W.M.; Wang, J.L. Investigation on the dynamic characteristics of a rotor-damper-casing coupling system under diving-climbing maneuver. *J. Sound Vib.* **2024**, *570*, 118094. [CrossRef]
2. Andrés, L.S. Force coefficients for a large clearance open ends squeeze film damper with a central feed groove: Experiments and predictions. *Tribol. Int.* **2014**, *71*, 17–25. [CrossRef]
3. Fu, C.; Zhang, K.F. A comprehensive study on natural characteristics and dynamic responses of a dual-rotor system with inter-shaft bearing under non-random uncertainty. *J. Sound Vib.* **2024**, *570*, 118091. [CrossRef]

4. Tarkashvand, A.; Golmohammadi, A. Stability and modal analysis of an unbalanced asymmetric multi-disk rotor system on bearings as viscoelastic substrate. *Arch. Appl. Mech.* **2022**, *92*, 2247–2271. [CrossRef]
5. Siew, C.C.; Hill, M.; Holmes, R. Evaluation of various fluid-film models for use in the analysis of squeeze film dampers with a central groove. *Tribol. Int.* **2002**, *35*, 533–547. [CrossRef]
6. Zhang, W.; Ding, Q. Elastic ring deformation and pedestal contact status analysis of elastic ring squeeze film damper. *J. Sound Vib.* **2015**, *346*, 314–327. [CrossRef]
7. Animasaun, I.L.; Shah, N.A.; Wakif, A.; Mahanthesh, B.; Sivaraj, R.; Koríko, O.K. *Ratio of Momentum Diffusivity to Thermal Diffusivity: Introduction, Meta-Analysis, and Scrutinization*, 1st ed.; Chapman and Hall/CRC: New York, NY, USA, 2022; p. 410.
8. Groves, K.H.; Bonello, P. Improved identification of squeeze-film damper models for aeroengine vibration analysis. *Tribol. Int.* **2010**, *43*, 1639–1649. [CrossRef]
9. Cao, J.; Dimond, T.; Allaire, P. Numerical analysis of flexible rotor with nonlinear bearings and squeeze film dampers. In *ASME 2014 International Mechanical Engineering Congress and Exposition*; American Society of Mechanical Engineers Digital Collection: New York, NY, USA, 2014.
10. Holmes, R. The damping characteristics of vibration isolators used in gas turbines. *J. Mech. Eng. Sci.* **1977**, *19*, 271–277. [CrossRef]
11. Holmes, R. The non-linear performance of squeeze-film bearings. *J. Mech. Eng. Sci.* **1972**, *14*, 74–77. [CrossRef]
12. Wang, X.J.; Han, Z.F.; Ding, Q. Influence of fluid inertia on dynamic characteristics of elastic ring squeeze film damper-rotor system. *J. Aerosp. Power* **2018**, *33*, 2981–2990.
13. Gu, Z.P.; Zhi, X.Z. Nonlinear analysis of a squeeze-film damper. *Mech. Eng.* **2003**, *25*, 38–41.
14. Gunter, E.J.; Barrett, L.E.; Allaire, P.E. Design of nonlinear squeeze-film dampers for aircraft engines. *J. Lubr. Technol.* **1977**, *99*, 57–64. [CrossRef]
15. Allaire, P.E.; Barrett, L.E.; Gunter, E.J. Variational method for finite length squeeze film damper dynamics with applications. *Wear* **1977**, *42*, 9–22. [CrossRef]
16. Cao, L.; Gao, D.P. Damping machanism of elastic ring squeeze film damper. *J. Vib. Eng.* **2007**, *20*, 584–588.
17. Cao, L.; Gao, D.P. Investigation on critical speed characteristics of elastic ring sfd-rotor system. *J. Propuls. Technol.* **2008**, *29*, 235–239.
18. Gu, J.L.; Wang, Q. Active vibration control of rotor-support system by the controlled SFDB. *Chin. J. Appl. Mech.* **1990**, *7*, 41–47.
19. Liu, F.J.; Yin, X.Q. Studies of Parameters Cooperated for Squeeze film damper. *Struct. Environ. Eng.* **1996**, *2*, 27–34.
20. Chu, F.L.; Tai, J.Y. Nonlinear vibration of a rotor system supported by the squeeze film damper. *Struct. Environ. Eng.* **1996**, *3*, 32–38.
21. Zhao, X.W.; Luo, G.H. Numerical Analysis of Effects of Static Eccentricity on Vibration Characteristics of Squeeze Film Damper. *J. Aerosp. Power* **2018**, *3*, 42–48.
22. Zhou, H.L.; Feng, G.Q. Damping mechanism of floating ring squeeze film damper. *J. Aerosp. Power* **2015**, *30*, 966–971.
23. Zhang, W.; Han, B.B.; Zhang, K.P.; Ding, Q. Dynamic analysis of a rotor system supported on squeeze film damper with air entrainment. *Int. J. Bifurc. Chaos* **2017**, *27*, 1750212. [CrossRef]
24. Rao, M.A.; Srinivas, J. Dynamics of rotors supported on fluid-film bearings using neural networks. *Proc. Inst. Mech. Eng. Part J J. Eng. Tribol.* **2001**, *215*, 149–155. [CrossRef]
25. Groves, K.; Bonello, P. An investigation into two alternative approaches for the identification of SFD bearings for aeroengine analysis. In Proceedings of the ASME 2011 Turbo Expo: Turbine Technical Conference and Exposition, Vancouver, BC, Canada, 6–10 June 2011; American Society of Mechanical Engineers Digital Collection; pp. 537–547.
26. Groves, K.; Bonello, P. Empirical identification of squeeze-film damper bearings using neural networks. *Mech. Syst. Signal Process.* **2013**, *35*, 307–323. [CrossRef]
27. Haobo, W.; Yulai, Z. Analysis on Influences of Squeeze Film Damper on Vibrations of Rotor System in Aeroengine. *Appl. Sci.* **2022**, *12*, 615.
28. Li, B.; Cheng, D.C. Experiment study on dynamic characteristics of elastic ring squeeze film damper rotor system. *Gas Turbine Exp. Res.* **2015**, *28*, 19–22.
29. Zhang, L.H.; He, L.D. Structure design of an integral elastic ring squeeze film damper and experiments on the rotor passing through critical speed. *J. Vib. Shock* **2019**, *38*, 72–78+108.
30. Sobol, I.M. Sensitivity estimates for nonlinear mathematical models. *Math. Model. Comput. Exp.* **1993**, *1*, 407–414.
31. He, K.; Yan, Z.; Xu, X.Y. Sobol' method-based global sensitivity analysis of isolated microgrid currents. *Autom. Electr. Power Syst.* **2018**, *42*, 99–106.